Phonon dispersion and phonon densities of states for ZnS and ZnTe*

N. Vagelatos, D. Wehe, and J. S. King

Department of Nuclear Engineering, The University of Michigan, Ann Arbor, Michigan 48104
(Received 21 December 1973)

Neutron scattering data are reported for II-VI zincblende crystals, which are believed to be of sufficient precision to refine earlier ZnS ambiguities and to provide a basis for model fitting comparable to existing III-V results. Valence shell models, including 9–12 parameters (VSM) and a variable shell charge extension (VCM), were fit to the data and used to generate phonon density of states and Debye temperatures. Very good fits to the neutron data were obtained, but no model was found that also predicts an accurate set of electric and mechanical constants. It is concluded that an unambiguous ionic charge Z cannot be assigned from the neutron results in either case.

I. INTRODUCTION

This paper reports phonon dispersion measurements and analyses for two zincblende II–VI compounds, ZnTe and ZnS. The measurements were undertaken to provide accurate "state of the art" data which could be used to test physical models for II–VI cubic systems, since most studies of partially covalent-bonded zincblende structures have been limited to III–V compounds.[1-3] The ZnTe data are new[4]; the ZnS data refine and add (finally, we hope) to earlier data,[5,6] particularly at the zone boundaries and in the optic mode region.

The conventional dipolar shell model[1,7] is apparently inadequate in several respects when applied to the zincblende semiconductor system. A 14-parameter tensor force model has been required to simultaneously fit neutron data and predict known physical constants, and some of these are not always realistic. Despite this

TABLE I. Measured frequencies (THz) for ZnTe.

[00ζ]				
q/q_{max}	*TA*	*LA*	*TO*	*LO*
0.0			5.30 ± 0.07	6.20 ± 0.05
0.1			5.24 ± 0.07	6.22 ± 0.05
0.2	0.75 ± 0.02	1.19 ± 0.02		6.24 ± 0.05
0.3	1.05 ± 0.02	1.72 ± 0.02	5.16 ± 0.06	6.16 ± 0.10
0.4	1.27 ± 0.02	2.23 ± 0.02		
0.5	1.44 ± 0.03	2.70 ± 0.02	5.11 ± 0.06	5.96 ± 0.05
0.6	1.52 ± 0.03	3.18 ± 0.04		
0.7	1.57 ± 0.04	3.55 ± 0.04	5.16 ± 0.08	5.75 ± 0.05
0.8	1.59 ± 0.04	3.92 ± 0.05		
0.9	1.61 ± 0.02	4.20 ± 0.05	5.20 ± 0.05	5.49 ± 0.08
1.0	1.62 ± 0.02	4.29 ± 0.05	5.21 ± 0.10	5.51 ± 0.10

[ζζζ]				
q/q_{max}	*TA*	*LA*	*TO*	*LO*
0.0			5.30 ± 0.04	6.20 ± 0.05
0.1			5.28 ± 0.04	6.20 ± 0.05
0.2	0.56 ± 0.02	1.18 ± 0.02		
0.3	0.77 ± 0.02	1.70 ± 0.02	5.16 ± 0.07	6.15 ± 0.10
0.4	0.95 ± 0.02	2.22 ± 0.02		
0.5	1.07 ± 0.02	2.66 ± 0.03	5.18 ± 0.05	5.90 ± 0.05
0.6	1.16 ± 0.02	3.10 ± 0.03		
0.7	1.21 ± 0.02	3.45 ± 0.04	5.12 ± 0.06	5.70 ± 0.05
0.8	1.25 ± 0.03	3.77 ± 0.03		
0.9	1.26 ± 0.03	3.95 ± 0.05	5.18 ± 0.07	5.41 ± 0.05
1.0	1.25 ± 0.02	4.06 ± 0.05	5.20 ± 0.09	5.39 ± 0.05

[ζζ0]					
q/q_{max}	*TA*	Σ_1A_2	Σ_1A_1	Σ_10_2	Σ_10_1
0.0					
0.1				5.30 ± 0.05	6.22 ± 0.05
0.2	0.77 ± 0.02	1.04 ± 0.02	1.69 ± 0.03		
0.3	1.05 ± 0.02	1.48 ± 0.02	2.41 ± 0.03	5.25 ± 0.05	5.92 ± 0.10
0.4	1.26 ± 0.03	1.83 ± 0.03	2.92 ± 0.04		
0.5	1.40 ± 0.03	2.11 ± 0.02	3.35 ± 0.05	5.17 ± 0.10	5.56 ± 0.10
0.6	1.50 ± 0.03	2.29 ± 0.05	3.65 ± 0.05		
0.7	1.57 ± 0.04	2.30 ± 0.05	3.98 ± 0.05	5.08 ± 0.10	5.50 ± 0.05
0.8	1.62 ± 0.04	2.15 ± 0.05	4.12 ± 0.05		
0.9	1.60 ± 0.04	1.80 ± 0.05	4.26 ± 0.05	5.13 ± 0.04	5.40 ± 0.05
1.0	1.62 ± 0.02	1.62 ± 0.02	4.29 ± 0.05		
0.55			3.53 ± 0.05		
0.65			3.85 ± 0.05		
0.75			4.01 ± 0.10		

TABLE II. Measured frequencies (THz) for ZnS.

[00ζ]				
q/q_{max}	*TA*	*LA*	*TO*	*LO*
0.0			8.30 ± 0.10	10.44 ± 0.15
0.1				
0.2	1.18 ± 0.02	1.94 ± 0.04	8.40 ± 0.10	10.46 ± 0.10
0.3	1.66 ± 0.02	2.80 ± 0.03		
0.4	2.05 ± 0.03	3.57 ± 0.03	8.63 ± 0.10	10.31 ± 0.10
0.5	2.33 ± 0.03	4.31 ± 0.03		
0.6	2.50 ± 0.04	4.98 ± 0.03	9.00 ± 0.10	10.11 ± 0.10
0.7	2.62 ± 0.05	5.55 ± 0.04		
0.8	2.67 ± 0.05	6.02 ± 0.06	9.25 ± 0.10	9.98 ± 0.10
0.9	2.68 ± 0.04	6.30 ± 0.05		
1.0	2.69 ± 0.04	6.34 ± 0.10	9.47 ± 0.10	9.90 ± 0.10

[ζζζ]				
q/q_{max}	*TA*	*LA*	*TO*	*LO*
0.0			8.30 ± 0.10	10.44 ± 0.15
0.1				
0.2	0.80 ± 0.02	1.80 ± 0.04	8.36 ± 0.10	10.46 ± 0.15
0.3	1.16 ± 0.02	2.68 ± 0.04		
0.4	1.45 ± 0.02	3.49 ± 0.05	8.50 ± 0.10	10.40 ± 0.10
0.5	1.68 ± 0.03	4.24 ± 0.04		
0.6	1.85 ± 0.04	4.80 ± 0.03	8.58 ± 0.10	10.28 ± 0.10
0.7	1.97 ± 0.04	5.24 ± 0.05		
0.8	2.08 ± 0.05	5.65 ± 0.06	8.63 ± 0.10	10.12 ± 0.15
0.9	2.10 ± 0.04	5.80 ± 0.08		
1.0	2.10 ± 0.04	5.85 ± 0.08	8.67 ± 0.10	10.10 ± 0.25

[ζζ0]					
q/q_{max}	*TA*	Σ_1A_2	Σ_1A_1	Σ_10_2	Σ_10_1
0.0				8.30 ± 0.10	10.44 ± 0.15
0.1					
0.2	1.16	1.72	2.85 ± 0.04	8.49 ± 0.10	10.41 ± 0.15
0.3	1.64	2.34	3.85 ± 0.04		
0.4	2.05	2.95	4.61 ± 0.04	9.03 ± 0.10	10.30 ± 0.15
0.5	2.38	3.30 ± 0.04	5.15 ± 0.06		
0.6	2.53	3.56 ± 0.06	5.50 ± 0.06	9.22 ± 0.10	10.06 ± 0.20
0.65			5.55 ± 0.06		
0.7	2.61	3.60 ± 0.06	5.67 ± 0.08		
0.75			5.83 ± 0.07		
0.8	2.65	3.35 ± 0.05	5.92 ± 0.07	9.05 ± 0.15	9.90 ± 0.10
0.9	2.69	2.90 ± 0.04	6.24 ± 0.08		
1.0	2.69 ± 0.04	2.69 ± 0.04	6.34 ± 0.10	9.47 ± 0.10	9.90 ± 0.10

TABLE III. Fitted valence parameters and corresponding tensor force constants at the "low-Z" (I and Ia) and "high-Z" (II and IIa) minima of ZnS and ZnTe. a denotes the least squares fits made using only the measured neutron data.

	ZnTe				ZnS			
	I	Ia	II	IIa	I	Ia	II	IIa
Valence parameters								
λ	10.130	9.474	18.150	13.030	13.680	13.140	23.420	23.340
$k'\theta$	0.991	0.995	0.259	0.783	0.273	0.051	−0.270	−0.172
$k'r\theta$	−0.544	−0.305	−1.033	−0.267	0.366	0.466	−1.157	−1.589
$k\theta$	−0.424	−0.366	−1.295	−0.903	0.391	0.630	−0.915	−1.015
$kr\theta$	0.901	0.868	1.772	1.604	0.250	0.568	2.354	2.579
dVI	1.012	0.754	0.614	0.110	0.172	0.117	0.516	0.628
dII	0.290	0.307	−0.903	−0.406	1.016	0.797	−0.603	−0.609
αVI	8.254	10.470	2.004	0.193	0.920	0.877	1.046	1.423
αII	0.719	1.040	6.709	4.575	4.974	6.532	4.388	4.520
ZII	−0.015	−0.011	1.983	1.297	−0.080	−0.065	1.818	1.892
Force constants								
α	−3.796	−3.466	−3.976	−2.922	−4.865	−4.313	−5.099	−5.265
β	−2.915	−2.606	−6.570	−4.108	−3.972	−3.682	−8.314	−8.336
α_2	0.917	0.807	0.660	0.648	0.010	0.186	0.366	0.634
ρ_2	0.266	0.296	−0.035	0.230	0.134	0.072	−0.226	−0.244
β_2	−0.037	−0.094	0.200	−0.068	−0.132	−0.118	0.318	0.403
τ_2	−0.037	−0.094	0.200	−0.068	−0.132	−0.118	0.318	0.403
a_2	−0.707	−0.653	−1.699	−1.358	0.143	0.152	−1.720	−1.892
r_2	−0.035	−0.020	−0.223	−1.112	0.160	0.277	−0.028	−0.034
b_2	−0.142	−0.144	−0.203	−0.228	−0.124	−0.239	−0.402	−0.439
t_2	−0.142	−0.144	−0.203	−0.228	−0.124	−0.239	−0.402	−0.439
ζ_2	0.117	0.053	0.188	0.036	0.158	0.109	0.189	0.134

fact, we have exploited the model in repeated fitting attempts to (a) corroborate the experience on III–V compounds; (b) determine possible improvements using a variable charge model (VCM), which allows shell charges to vary with shell displacement[8]; and (c) obtain the best possible interpolation formulas to extract phonon densities $g(\nu)$. We assume, as we have previously, that a 12-parameter valence shell model (VSM) is essentially equivalent to the usual 14-parameter tensor force model.[6]

II. EXPERIMENTAL

Dispersion curves were obtained for phonons propagating in the [001], [110], and [111] symmetry directions. The Brockhouse constant-Q method for triple axis crystal spectrometers (TACS) was used throughout.[9] Targets were maintained at room temperature, and only down-scattering was observed. Initial data were taken at the 2 MW Michigan FNR; final data were taken on the HB-3 and HB-4A spectrometers at the HFIR (ORNL).

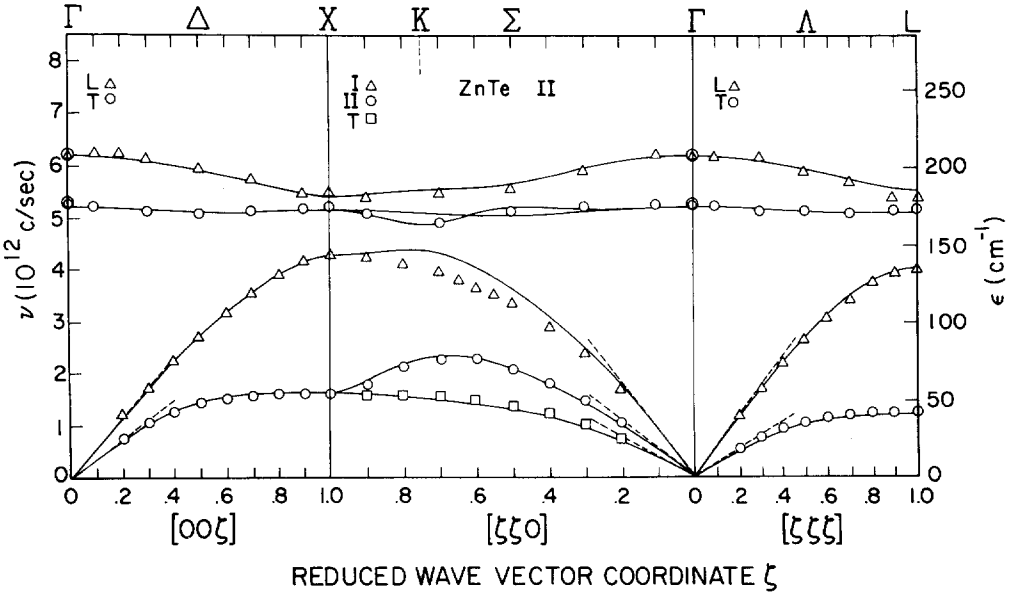

FIG. 1. Dispersion data and "best fit" 10-parameter VSM model for ZnTe. The two enlarged points at Γ are optical data.

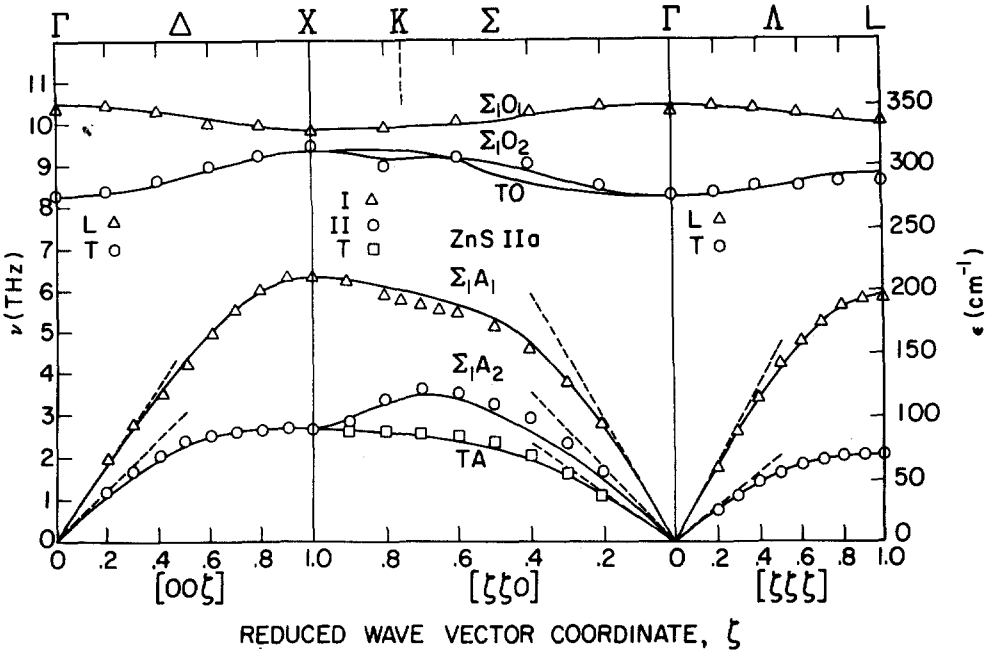

FIG. 2. Dispersion data and "best fit" 10-parameter VSM model for ZnS.

The ZnS targets were a 0.5 cm^3 twin-free sample cut from a twinned, natural crystal and an 18 cm^3 twinned, polymorphic sample[10] grown by vapor deposition. The 0.5 cm^3 target was used for all acoustic branch measurements while the 18 cm^3 target was used for the optic modes and for acoustic mode comparison tests. The ZnTe target was a 7 cm^3 composite of 16 single, twinned crystals, individually oriented by neutron diffraction,[2,10] and cemented together by Eastman 404 quick-set adhesive.

The final data are listed in Tables I and II. The errors listed are the statistical uncertainties assigned to individual frequencies and are generally 1%–2%. The contribution of systematic errors is believed to be negligible as a result of repeated cross comparison of calibration and target alignment. Resolution effects were minimized by careful choice of the scans. The zone center optic frequencies are in excellent agreement with optical measurements,[11–13] and the acoustic frequencies near the zone center are generally in very good agreement with the velocities of sound determined from the elastic constants.[14]

III. MODEL CALCULATIONS

The models used included a 10- and a 12-parameter VSM, a 9-parameter VSM with Z fixed by ionicity predictions,[15,16] and an 11-parameter VCM. The valence notation and cell geometry are the same as in our previous paper.[6] The shell model treatment is also the same, except that more exact expressions for Z^* and α_0 are used, retaining polarizability coupling terms.[17] The VCM follows the expanded equations of motion as in reference.[8]

Least square fitting to the data along $[00\zeta]$ and $[\zeta\zeta\zeta]$ was done using several options: (a) with neutron data alone (denoted by subscript "a," Table III); (b) adding electric parameters e_{14} and ϵ_0 as fitting data (denoted by absence of subscript, Table III); (c) with fixed charge Z.

Based on numerous trials, it was found that neither the VCM nor the 12-parameter VSM made significant improvements over the 10-parameter VSM. Fixing Z at 0.25 for ZnTe and at 0.45 for ZnS, corresponding to reasonable ionicity choices, gave only a slightly inferior fit to the neutron data. The 10-parameter VSM was, nevertheless, felt to be the best overall model and was

TABLE IV. Physical parameters of ZnS and ZnTe calculated from VSM force constants compared to observed values. The measured values are obtained from Ref. [14].

	ZnTe					ZnS				
Parameter	I	Ia	II	IIa	Observed	I	Ia	II	IIa	Observed
$C_{11}\times10^{-11}d/cm^2$	7.389	7.235	7.170	6.999	7.12	10.89	10.62	10.93	10.96	10.45
C_{12} "	4.603	4.143	4.706	4.357	4.07	7.183	6.826	7.20	6.357	6.53
C_{44}^E "	2.450	2.740	2.727	3.076	3.12	3.355	3.559	4.249	4.228	4.613
C_{44}^D "	2.451	2.742	2.728	3.377	3.12	3.383	3.607	4.275	4.298	4.643
ϵ_0	10.34	23.42	7.495	3.57	10.1	8.944	17.64	6.78	7.675	8.3
$\alpha_0\times10^{24}cm^3$	10.27	11.97	9.284	6.261	10.21	6.86	8.00	6.231	6.516	6.7
e_{14} esu/cm^2	8,374	16,610	8,310	92,470	8,400	44,610	82,790	42,440	−73,550	44,100
Z^*	−0.633	−0.377	0.762	0.835	0.653	0.776	0.615	0.896	0.868	0.88

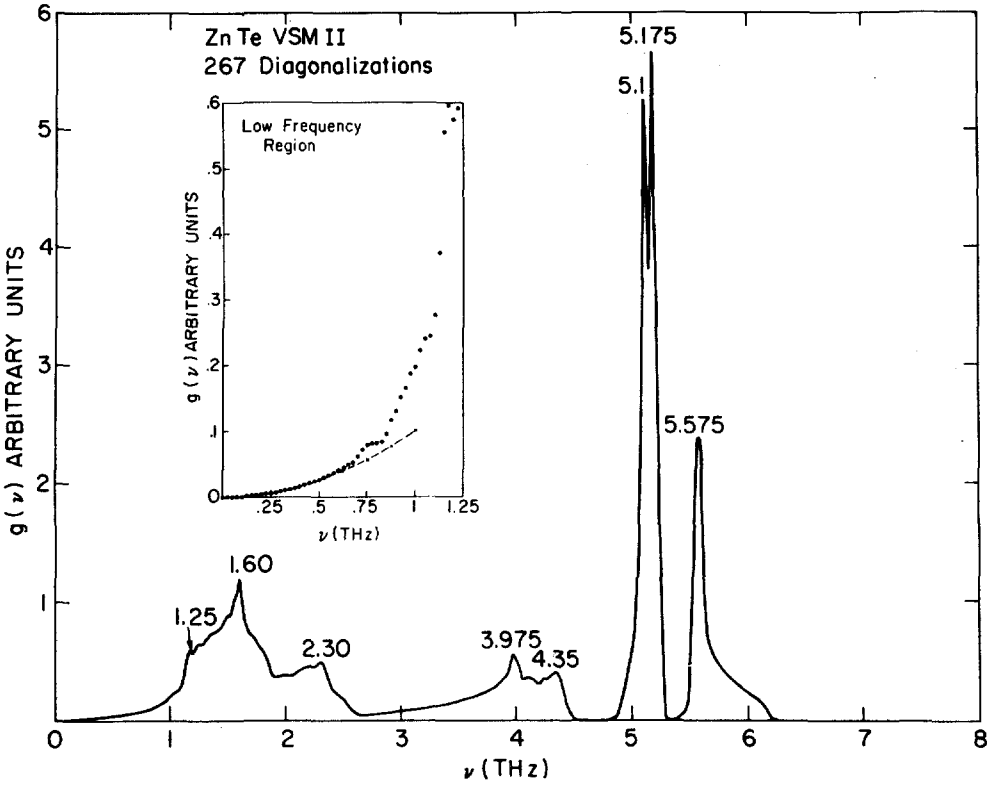

FIG. 3. Phonon density of states for ZnTe–II.

used for the final results.

Two different convergent parameter sets (minima of the fitting index ζ^2) were found for both crystals, one characterized by a nearly zero negative ionic charge Z [models I, I(a)] and the other by a large positive ionic charge approaching +2.0 [models II, II(a)]. The valence parameters and corresponding tensor force constants are given in Table III (ζ^2 for subscripted and unsubscripted models are different). Figure 1 shows the degree of fit for ZnTe–II and Fig. 2 shows the case of ZnS-IIa. Physical parameters calculated from all these models are compared with values given by Berlincourt[14] in Table IV.

The density of states and Debye temperatures were obtained from the ORNL GNU code which uses the extrapolation procedure of Gilat and Raubenheimer,[18] adapted by David L. Price for zincblende symmetry and modified by us to fit our model notation. The fitted shell model parameters are the required input. Following the precept that the most reliable $g(\nu)$ is obtained from the model most accurately reproducing the dispersion curves, independent of the results of Table IV, we considered ZnTe–II and ZnS–II(a) the most appropriate inputs. The $g(\nu)$ for ZnTe–II, using 267 diagonalizations (crude mesh) is shown in Fig. 3. Figure 4 gives $g(\nu)$ for ZnS–II(a), with 389 diagonalizations. The variation of θ_D with temperature is shown for ZnTe–II by the solid curve of

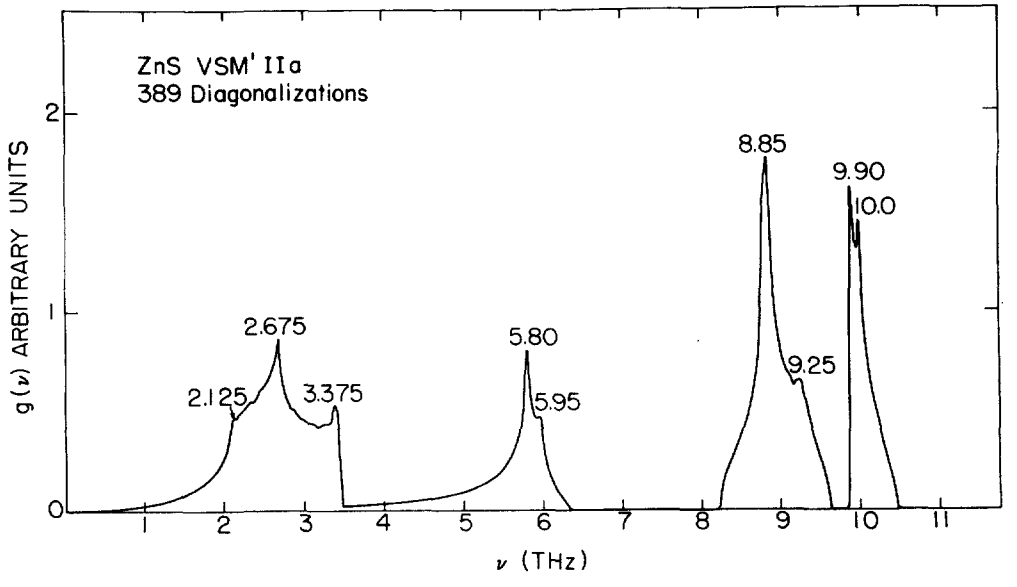

FIG. 4. Phonon density of states for ZnS-IIa.

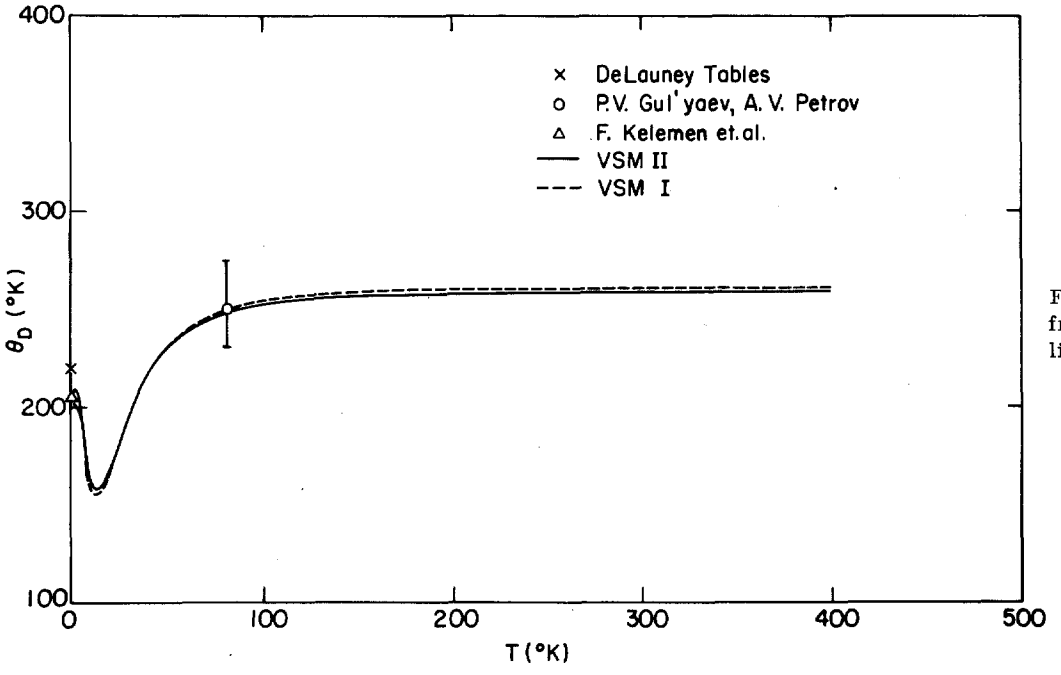

FIG. 5. Debye temperatures from ZnTe models and published specific heat data.

Fig. 5, and for ZnS–II(a) by the solid curve of Fig. 6. To show model sensitivity, the dashed curves corresponding to ZnTe–I and ZnS–I, respectively, are also shown. The calculations below 2 °K could be in error due to crudeness of mesh, and hence the reversed slopes there are questionable. The data points shown are measurements available in the literature.[19–24] The C_v in all cases shows the expected temperature dependence. For ZnTe–II and ZnS–II(a), these extrapolate near melting temperature to 5.95 and 5.94 cal/mole °K, respectively.

IV. DISCUSSION

The present ZnS data are, within the errors quoted in both experiments, in agreement with Bergsma's inverse Be filter frequencies for the optic modes.[5] The largest divergence occurs for LO(X) and is 0.25 THz. The present data are in significant disagreement both with our own earlier results[6] and with Bergsma's conventional optic data, but fortify the precision of Bergsma's Be technique. We believe, also, the several reported un-

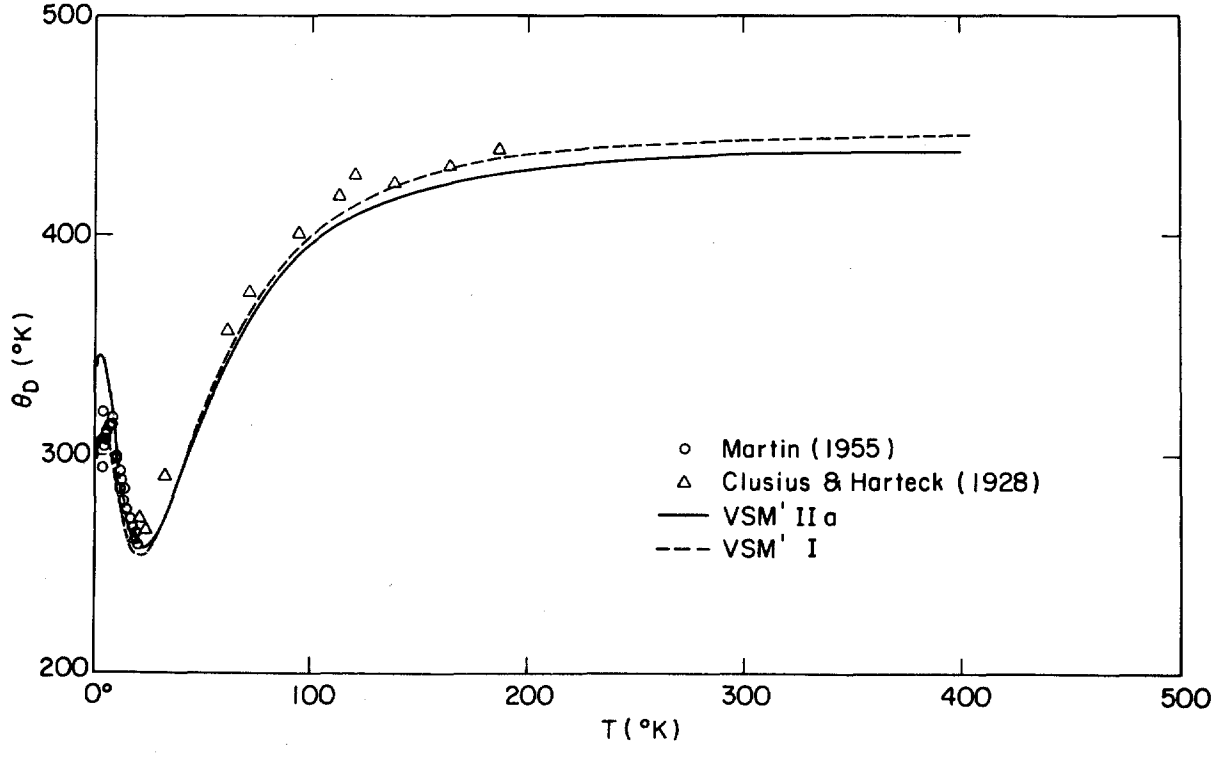

FIG. 6. Debye temperatures from ZnS models and published specific heat data.

certainties for points near LA(X) are now accurately resolved. If these frequencies are to be believed, then the impressive multiphonon table given by Vetelino[25] would not be satisfied.

Several conclusions can be drawn from our shell model fitting attempts. First, it is clear that our model cannot be used to establish an unambiguous ionic charge Z. We believe this will also be true for any other shell model in the dipole approximation. Second, the "high Z" models appear to require unphysical charge assignments for the deformation charges d_{II} and d_{VI}, the sums being small or negative, by virtue of large negative d_{II} assignments. Third, the "small Z" fits for ZnTe require a negative Z^*. It is patently clear that Z^* is positive for ionic salts such as NaI, and it was anticipated that this would be true certainly for ZnS and probably for ZnTe. Fourth, unless e_{14} and ϵ_0 are forced as fitting data, all the models are completely unable to fit both parameters simultaneously, independent of the magnitude of Z. Thus an excellent fit to the neutron data does not provide, in general, satisfactory modelling of electric parameters.

The phonon densities and resulting Debye temperatures behave rather differently for ZnTe and ZnS. For ZnTe, θ_D appears quite model insensitive, yet there is a significant shift in critical points in $g(\nu)$ between ZnTe–I and ZnTe–II. While $g(\nu)$ for ZnTe–II shows good agreement with our observed critical frequencies, this is not the case for ZnTe–I; most of the latter acoustic peaks shift by as much as 0.2 THz. By contrast, $g(\nu)$ for both ZnS–II(a) and ZnS–I show close agreement with each other and with our observed critical points in the acoustic region but not for the optic region. Furthermore θ_D is more model sensitive as seen in Fig. 6.

These differences correlate qualitatively with the data fitting disagreements for each model. In the case of ZnS, this is due primarily to the large "bump" in $\Sigma_1 0_1$ characteristic of "low Z" shell model results. This "bump" is in obvious disagreement with the measured frequencies.

Based on the $g(\nu)$ and θ_D characteristics for both ZnTe and ZnS, we are led to select the "high Z" models, ZnTe–II and ZnS–II(a). The agreement with published data, though scant, appears to support this choice, although it would be desirable to repeat the ZnS data at low temperature to obtain the most precise low temperature moments of $g(\nu)$.[26]

ACKNOWLEDGMENTS

We wish to express our gratitude particularly to Dr. Harold Smith and other members of the Oak Ridge National Laboratory Solid State Division, not only for making the HFIR facilities available but for numerous guiding comments. We also wish to acknowledge the many enlightening discussions and stimulation provided by Dr. Lee Feldkamp concerning the physics of shell model variations. Finally, we thank Dr. D. C. Reynolds and Dr. C. Kikuchi, for the gifts of target specimen.

*Work supported by the National Science Foundation under NSF Grant GK-12492.

[1]G. Dolling and J. L. Waugh, in *Lattice Dynamics*, edited by R. F. Wallis (Pergamon, Oxford, 1965), p. 19.
[2]J. L. Yarnell, J. L. Warren, R. G. Wenzel, and P. J. Dean, in *Neutron Elastic Scattering* (IAEA, Vienna, 1968).
[3]D. L. Price, J. M. Rowe, and R. M. Nicklow, Phys. Rev. **B 3**, 1268 (1971).
[4]N. Vagelatos, J. S. King, and L. A. Feldkamp, Bull. Am. Phys. Soc. **18**, 313 (1973).
[5]J. Bergsma, Phys. Lett., **A 32**, 324 (1970); J. Bergsma, "Lattice Dynamics of Magnesium Stanide and Zinc Blende," Reactor Centrum, Nederland Report No. RCN-121, 1970.
[6]L. A. Feldkamp, D. K. Steinman, N. Vagelatos, J. S. King, and G. Venkataraman, J. Phys. Chem. Solids **32**, 1573 (1971).
[7]A. D. B. Woods, W. Cochran, and B. N. Brockhouse, Phys. Rev. **19**, 980 (1960).
[8]L. A. Feldkamp, J. Phys. Chem. Solids **33**, 711 (1972).
[9]B. N. Brockhouse, S. Hautecler, and H. Stiller, edited by R. Strumane *et al.*, *Interaction of Radiation with Solids* (North-Holland, 1963).
[10]N. Vagelatos, thesis, The University of Michigan, 1973.
[11]J. C. Irwin, L. LaCombe, J. Applied Phys. 41, 1444 (1971).
[12]O. Brafman, S. S. Mitra, Phys. Rev. 171, 931 (1963).
[13]S. S. Mitra, O. Brafman, W. B. Daniels, R. K. Crawford, Phys. Rev. **168**, 942 (1939).
[14]D. Berlincourt, H. Jaffe, L. R. Shiozawa, Phys. Rev. **129**, 1009 (1963).
[15]C. A. Coulson, L. B. Redei, D. Stocker, Proc. R. Soc., Lond. **270**, 352 (1962).
[16]J. C. Phillips, Rev. Mod. Phys. **42**, 317 (1970).
[17]R. A. Cowley, Proc. R. Soc., **A 268**, 121 (1963).
[18]G. Gilat and L. J. Raubenheimer, Phys. Rev. **44**, 390 (1966).
[19]D. L. Martin, Philos. Mag. **46**, 751–758 (1955).
[20]F. Kelemen, D. Niculescu, and E. Cruceanu, Phys. Status Solidi **11**, 865–872 (1965).
[21]P. V. Gul'yaev and A. V. Petrov, Sov. Phys.–Solid State **1**, 330–334 (1959).
[22]K. Clusius and P. Harteck, Z. Phys. Chem. **134**, 243 (1928).
[23]J. De Launay, J. Chem. Phys. **22**, 1676 (1954).
[24]A. F. Demidenko, *et al.*, Izv. Akad. Nauk SSSR Neorg. Mater. **5** (1) 158–160 (1969).
[25]J. F. Vetelino, S. S. Mitra, and Namjoshi, Phys. Rev. **B 2**, 967 (1970).
[26]G. Gilat and R. M. Nicklow, Phys. Rev. **143**, 487 (1966).